Talanta 118 (2014) 54–60

Contents lists available at ScienceDirect

Talanta

journal homepage: www.elsevier.com/locate/talanta

Multifunctional AS1411-functionalized fluorescent gold nanoparticles for targeted cancer cell imaging and efficient photodynamic therapy

Jun Ai [1], Yuanhong Xu [1], Baohua Lou, Dan Li, Erkang Wang *

State Key Laboratory of Electroanalytical Chemistry, Changchun Institute of Applied Chemistry, Chinese Academy of Sciences, Changchun, Jilin 130022, PR China

ARTICLE INFO

Article history:
Received 5 June 2013
Received in revised form
20 September 2013
Accepted 23 September 2013
Available online 9 October 2013

Keywords:
Fluorescent gold nanoparticles
AS1411-functionalized
N-methylmesoporphyrin IX
Cell imaging
Photodynamic therapy

ABSTRACT

Herein, one multifunctional AS1411-functionalized fluorescent gold nanoparticles (named NAANPs) is synthesized and successfully applied for both targeted cancer cell imaging and efficient photodynamic therapy (PDT). The NAANPs are obtained by functionalizing the gold nanoparticles with AS1411 aptamer and then bound with one porphyrin derivative N-methylmesoporphyrin IX (NMM). Using HeLa cells over expressing nucleolin as representative cancer cells, the formed NAANPs can target to the cell surface via the specific AS1411-nucleolin interaction, which can discriminate the cancer cells from normal ones (e.g. HEK293) unambiguously. That the fluorescence intensity of NMM increased significantly upon binding to AS1411 G-quadruplex makes the NAANPs appropriate fluorescence reagent for cell imaging. Meanwhile, NMM can also be used as a photosensitizer, thus irradiation of the NAANPs by the white light from a common electric torch can lead to efficient production of cytotoxic reactive oxygen species for establishing a new type of PDT to cancer cells. Gold nanoparticles play the roles of both carrier and enhancer of the functional groups onto the cells. In addition, they not only possess inherently certain cytotoxicity to the cancer cells, but also boost the cellular uptake of the fluorescent groups. As a result, the efficiency of both the targeted cell imaging and PDT could be ensured.

1. Introduction

With the tremendous development of nanotechnology, a variety of nanomaterials, gold nanoparticles in particular, have provided many promising nanoplatforms for cancer imaging and therapy [1–3]. Because of their unique physical and chemical properties, as well as simple synthesis and surface modification, gold nanoparticles could preferentially accumulate in cancer cells [4], and carry the detection signal or drugs for monitoring and treatment of the cancer [5]. Recently, to realize “green chemistry” that requires low toxicity but high activity, directly importing biological and biomimetic molecules into gold nanoparticles has been attracting increasing attention and was considered to be a desirable choice to develop non-invasive strategies for future cancer therapy [4]. A number of biomolecules can be loaded to create a nano-bioconjugate with multifunctional capabilities [6]. Such multifunctional gold nanoparticles containing targeting moieties, imaging labels, and therapeutic agents would lead to a critical thrust towards improving targeted therapeutic efficacy with reduced side effects [4,5]. Even though some progress has been made, it is still a promising field that expects much more effort and exploration.

AS1411 is a 26-base guanine-rich oligonucleotide, commonly known as anti-nucleolin aptamer, which could form a stable dimeric G-quadruplex structure to specifically bind the target nucleolin receptors over-expressed on the cancer cells [7,8]. Because the normal cells lack or have lower levels of the nucleolin receptors on the plasma membrane, nucleolin could be regarded as tumor biomarker to distinguish cancer cells from normal ones [8]. Thus the AS1411-nucleolin interaction could be utilized as a strategy to mediate highly specific and effective targeted therapeutic agents to cancer cells [9]. It was demonstrated that the AS1411 aptamer could enhance the uptake of certain nanoparticles in cancer cells such as MCF-7 and HeLa cells [10,11] than in normal ones. Moreover, it was reported that the unique structure of G-quadruplex DNA enabled it to bind to various porphyrin derivatives such as protoporphyrin IX, N-methylmesoporphyrin IX (NMM), etc. [12]. Generally, the porphyrin derivatives are weakly fluorescent by themselves in aqueous solution [13], while exhibit a dramatic fluorescence enhancement upon the binding to G-quadruplex DNA [14]. Although the AS1411-porphyrin binding

Abbreviations: AS1411-NMM, AS1411 combined with NMM; CD, circular dichroism; LSCM, laser scanning confocal microscope; MTT, 3-[4,5-dimethylthiazol-2-yl]-2,5-diphenyl tetrazolium bromide; NAANPs, AS1411-functionalized fluorescent gold nanoparticles; NMM, N-methylmesoporphyrin IX; PBS, phosphate buffered saline; PDT, photodynamic therapy; ROS, reactive oxygen species; TCEP, tris(β-chloroethyl)phosphate; TEM, transmission electron microscope

* Corresponding author. Tel.: +86 431 85262003; fax: +86 431 85689711.
E-mail address: ekwang@ciac.jl.cn (E. Wang).

[1] Jun Ai and Yuanhong Xu contributed equally to this work.

0039-9140/$ - see front matter © 2013 Elsevier B.V. All rights reserved.
http://dx.doi.org/10.1016/j.talanta.2013.09.062

based fluorescent assay have been widely studied for detection of metal ions [14,15], amino acids [16], DNA [17], etc., application in cancer cell imaging has just been tested [18]. Furthermore, AS1411-porphyrin functionalized fluorescent gold nanoparticles for targeted cell imaging were scarcely reported until now.

It is also worth noticing that the porphyrin derivatives can also be used as photosensitizers in photodynamic therapy (PDT) of cancer [19]. PDT is an attracting light-activated therapeutic modality for cancer treatment. In PDT, irradiation of a photoactive drug (i.e. a photosensitizer) with appropriate wavelengths of light would produce highly cytotoxic reactive oxygen species (ROS) to destroy cancerous cells [20,21]. However, many existing hydrophobic photosensitizers are with poor or limited solubility in aqueous solution, which would impair the systemic biodistribution and reduce the quantum yields of ROS [20,22]. In addition, pure photosensitizers exhibited limited selectivity towards cancer cells, which could lead to nonspecific photodamage of normal tissue [20]. To overcome these limitations, some nanoparticles-based platforms have been developed for photosensitizer drug delivery [20]. On one hand, such platform could keep the activity and stability of the photosensitizers in aqueous solution; on the other hand, the nanoparticles themselves could be further functionalized with targeting moieties for cancer-specific PDT [20]. Even so, for PDT using porphyrin derivatives as photosensitizers, simultaneous fluorescent cell imaging was still difficult to be achieved because of the low fluorescence intensity of free porphyrin derivative molecule. Therefore, the porphyrin derivatives (e.g. NMM) can both be fluorescence-enhanced by the AS1411 G-quadruplex but also be applied as photosensitizers motivated us to design one new functionalized fluorescent gold nanoparticles for both targeted imaging and efficient PDT to cancer cells.

Herein we present the synthesis and application of one gold nanoparticles that are modified with the AS1411 aptamer and followed being conjugated with one porphyrin derivative NMM (named NAANPs). Due to the specific interaction between AS1411 and the over-expressed nucleolin on some cancer cells surface, the NAANPs could targetedly bind to the nucleolin expressed on tumor cells such as HeLa cells (human cervical cancer cells) for both cell imaging and PDT purposes. The structures and spectroscopic properties of NAANPs were characterized by transmission electron microscope (TEM), UV and fluorescence assays. Laser scanning confocal microscope (LSCM) was carried out to study the cell uptake of NAANPs as well as the targeted bioimaging. Both LSCM and 3-[4,5-dimethylthiazol-2-yl]-2, 5-diphenyl tetrazolium bromide (MTT) assay were applied to show the cytotoxicity of NAANPs to the HeLa cells as well as the PDT efficacy.

2. Experimental

2.1. Chemicals

$HAuCl_4$ and MTT were obtained from Sigma-Aldrich (USA). Tris (β-chloroethyl)phosphate (TCEP) was purchased from Fluka (Buchs, Switzerland). The oligodeoxynucleotides used in the present study were SH-AS1411, an antiproliferative G-rich oligodeoxynucleotides whose sequence is 5′-(GGTGGTGGTGGTTGTGGTGGTGGTGGTTTSH)-3′, and were synthesized by Shanghai Sangon Biotechnology Co. Ltd. (Shanghai, China). NMM was purchased from Frontier Scientific (Logan, Utah, USA). HeLa cells were obtained from the American Type Culture Collection (Manassas, VA) and maintained in DMEM supplemented with 10% standard fetal bovine serum (HyClone Laboratories, UT) at 37 °C and in 5% CO_2. 35 mm glass chamber slides were purchased from Hangzhou Sanyou Biotechnology Co. Ltd. (Hangzhou, China). Citric acid and all chemicals of analytical grade were used as received without further purification. Stock solutions of 100 mM phosphate buffered saline (PBS) (pH=7.4) was also prepared. All the solutions were prepared by using distilled water and stored at 4 °C before use.

2.2. Apparatus and measurements

A XL30 ESEM scanning UV/vis absorption spectra were collected by a CARY 500 UV/vis/near-IR spectrophotometer (Varian Inc., USA). Fluorescence measurements were recorded at room temperature using a LS 55 luminescence spectrometer (Perkin-Elmer Instruments, U.K.). TEM images were obtained with a FEI TECNAI G2 transmission electron microscope (Eindhoven, Netherlands) operating voltage of 120 kV. The samples for TEM characterization were prepared by placing a drop of sample solution on carbon-coated copper grid and dried at room temperature.

2.3. Synthesis of the multifunctional gold nanoparticles

The gold nanoparticles of 13 nm diameter were synthesized by the citrate acid reduction method [23,24]. Thiolmodified AS1411 DNA was activated with two equivalents of TCEP. TCEP-activated thiolmodified AS1411 DNA and gold nanoparticles were mixed in 20 mM Tris–HCl buffer (pH=7.4) containing 100 mM KCl and stirred at room temperature for 24 h or longer. The solution was kept at 4 °C for another 24 h, and the AS1411-functionalized gold nanoparticles were purified by centrifugation and removal of supernatant before use [25]. The purified AS1411-functionalized gold nanoparticles were dissolved in 50 mM PBS buffer containing 0.1 M KCl to reach the stock concentration. Then the NMM was added and bound with AS1411-protected gold nanoparticles to form the final NAANPs. Stock solutions of NAANPs in 50 mM PBS containing 0.1 M KCl were prepared at 10 μM for further UV, fluorescence, TEM and circular dichroism (CD) characterizations as well as applications.

2.4. The intracellular uptake of NAANPs and bioimaging

HeLa cells (10^6 cells per sample) were plated onto 35 mm glass chamber slides. NAANPs solutions at 10 nM in DMEM were then freshly prepared and placed over the cells for 1 h at 37 °C. All cells were washed with PBS buffer three times at room temperature to remove free and physically absorbed NAANPs, followed by nucleus staining with Hoechst 33342 if needed. After that, the fluorescence images of the cells were taken using the LEICA TCS SP2 Laser Scanning Confocal Microscope (Leica Microsystems Heidelberg GmbH, Germany) with a 100 × oil immersion objective. The NAANPs were excited with 405 nm and Hoechst 33342 with UV. The normal HEK-293 cells were treated with the same procedure and used as control for binding specificity study.

2.5. MTT assays

MTT assays were used to evaluate the NAANPs doses and light illumination on the viability of the HeLa cells. The cells were treated with various concentrations of NAANPs (0, 1, 2, 5, 10 and 20 nM) in fresh DMEM for 24 h. Another same series of NAANPs-cultured cells was also prepared in the same concentration order but were additionally exposed to illumination of white light for 30 min. Treated cells were washed with PBS buffer before the addition of DMEM containing MTT (10 μL, 5 mg mL^{-1}) and further incubated at 5% CO_2, 37 °C for 4 h. Then, the MTT containing medium was added with 100 μL DMSO to solubilize the formazan crystals precipitate. Viability of untreated control cells was arbitrarily defined as 100%. Finally, the absorption at 490 nm of each

well was measured by an EL808 ultramicroplate reader (Bio-TEK Instrument, Inc., Winooski, VT, USA). The cell viability was reported relative to the absorbance of the untreated control (viability of control = 1).

2.6. PDT experiment

To test the PDT effects, a common electric torch with white light were applied to illuminate each NAANPs-treated cell sample for 30 min, respectively. The incoming illumination was with wide illumination (0–72°) and azimuthal angle ranges (0–360°). The illuminated cell samples were then used for further MTT assays and LSCM imaging. To characterize the light source, 1830-C Optical Power Meter (Newport Corp., USA) was used to detect the light intensity.

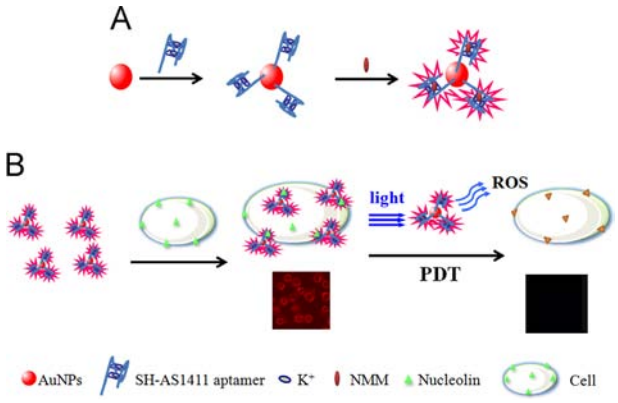

Fig. 1. Scheme of (A) synthesis of the NAANPs by functionalizing with AS1411 aptamer and bound with NMM and (B) utilization for targeted cell imaging and PDT to cancer cells over-expressed with nucleolin on the cell surface.

2.7. CD experiment

The CD spectra of 10 μM AS1411 aptamer in the absence or presence of 100 mM K^+ and 10 μM NAANPs in the presence of 100 mM K^+ was measured by recording from 210 to 330 nm on a J-820 circular dichroism spectropolarimeter (JASCO Pty Ltd., Japan) with a 1 cm path-length cuvette, 0.1 nm data pitch, scan speed of 200 nm min^{-1}, response time of 0.5 s. The optics was continuously flushed with dry nitrogen before and during the experiments. An average of three scans was taken to obtain a good signal to noise ratio.

3. Results and discussion

3.1. Characterization of the NAANPs

As shown in Fig. 1A, the citric acid-templated gold nanoparticles were mixed with SH-AS1411 aptamer to form the AS1411-functionalized gold nanoparticles through the Au–S bond. Due to the presence of K^+, G-quadruplex was formed and can be used to subsequently bind to NMM. The UV–vis spectra of citric acid-templated gold nanoparticles in aqueous solution and AS1411-functionalized gold nanoparticles in 50 mM PBS containing 0.1 M KCl are shown in Fig. 2A. The optical UV absorbance peak at 520 nm was consistent with that of gold nanoparticles at size of around 13 nm [23]. While functionalized with AS1411 aptamer, a modest shift (from 520 to 525 nm) in the surface plasmon band was observed. The shift was possibly due to the AS1411 modification [26]. To confirm the secondary structure of AS1411 conjugated in the NAANPs, CD experiment was performed. As shown, for 10 μM AS1411 in the absence of K^+ (Fig. 3a), no obvious CD signal was obtained. While in the presence of 100 mM K^+, both 10 μM AS1411 (Fig. 3b) and 10 μM NAANPs (Fig. 3c) showed CD spectrum

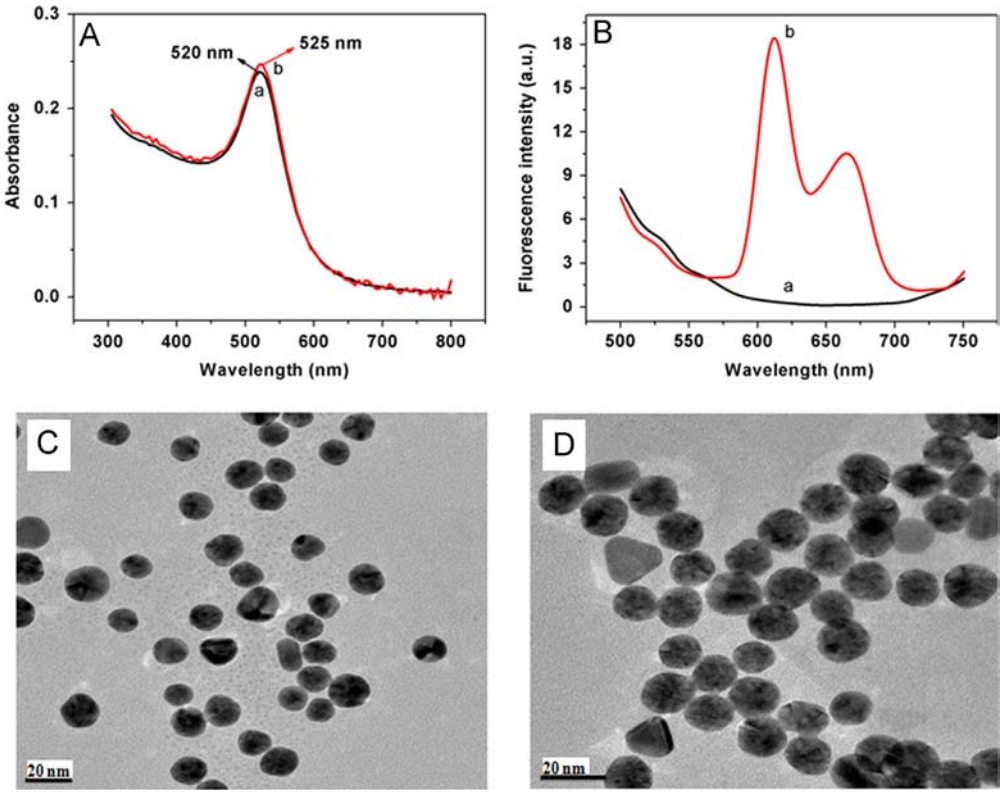

Fig. 2. (A) UV–vis spectra of (a) 10 nM citric acid-templated gold nanoparticles in aqueous solution and (b) 10 nM AS1411-functionalized gold nanoparticles in 50 mM PBS containing 0.1 M KCl, respectively; (B) fluorescence spectra of (a) 10 nM NMM and (b) 10 nM NAANPs in 50 mM PBS buffer (pH = 7.4) containing 100 mM KCl, respectively. Excitation wavelength was set at 405 nm; TEM images of (C) citric acid-templated gold nanoparticles and (D) AS1411-functionalized gold nanoparticles.

characterized by a positive maximum at 264 nm and a negative minimum at 240 nm. In addition, no obvious CD signal difference was observed between each other. It was indicative of the formation of K^+-stabilized quadruplexes for AS1411 in the NAANPs, which were with parallel conformation [27]. Moreover, both conjugation to the gold nanoparticles and combination with NMM would not influence much of the secondary structure of AS1411. TEM was also used for further characterizing the size and shape of both the citric acid-templated gold nanoparticles (Fig. 2C) and AS1411-functionalized gold nanoparticles (Fig. 2D). As shown, the gold nanoparticles were both monodispersed with a narrow size distribution (13–15 nm). Upon functionalization with AS1411, the average size did not change much but the particles became relatively uniform. It can be confirmed that although the AS1411 functionalization could endow the gold nanoparticles with some new properties, it would not surely influence much on the particle size distribution of the gold nanoparticles, the intrinsic properties of gold nanoparticles could be still kept for further applications. Accordingly, the formed AS1411 quadruplexes in the NAANPs could be used to target to the nucleolin over-expressed on the cell surface.

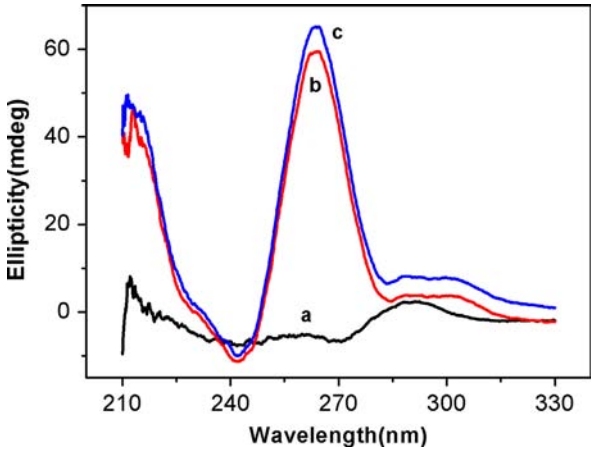

Fig. 3. CD spectra of 10 μM AS1411 aptamer in the (a) absence and (b) presence of 100 mM KCl, and (c) 10 μM NAANPs in the presence of 100 mM KCl.

To further confirm the target ability of the NAANPs to the nucleolin over-expressed cell surface, HeLa cells were either incubated with the 10 nM citric acid-templated gold nanoparticles or 10 nM NAANPs for 1 h at 37 °C and 5% CO_2, and then the treated cells were characterized by TEM. From the TEM images of these cells (see Fig. S1 in Supporting information), relatively fewer citric acid-templated gold nanoparticles exhibited on the cells (Fig. S1A), but large amount of NAANPs were observed being accumulated onto the cells (Fig. S1B). The comparison results demonstrated that the AS1411 aptamer could enhance the uptake of the gold nanoparticles into the cancer [10,11] cells due to the specific interaction between AS1411 and the nucleolin.

To confirm the fluorescent enhancement of NMM in the presence of AS1411 G-quadruplex formed on NAANPs, fluorescence spectra were collected for NMM and NAANPs 50 mM in PBS containing 100 mM KCl. As can be seen in Fig. 2B, upon excitation at wavelength at 405 nm, NMM at 10 nM was weakly fluorescent by itself (curve *a* in Fig. 2B), However, dramatic fluorescence enhancement with emission maximum at 612 nm was obtained for the NAANPs (curve *b* in Fig. 2B) at the same concentration.

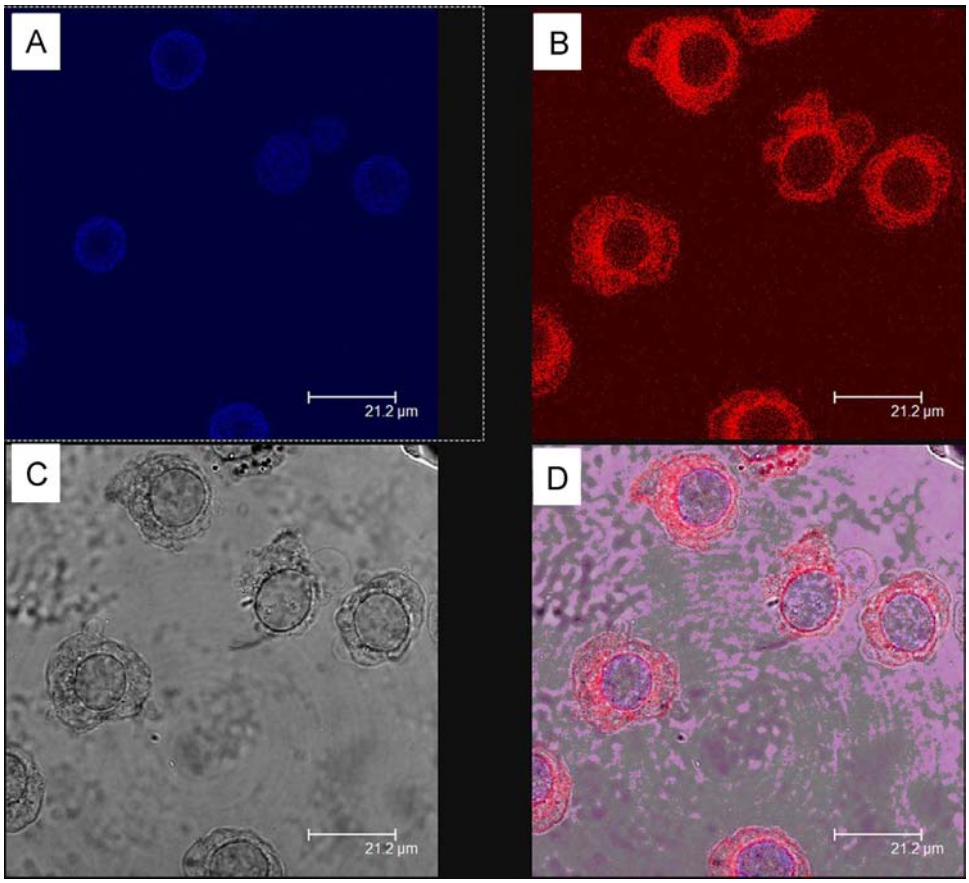

Fig. 4. LSCM images of HeLa cells incubated with 10 nM NAANPs for 1 h at 37 °C. (A) Fluorescence image with Hoechst 33342 nuclear staining (blue); (B) fluorescence image with NAANPs staining (red); (C) bright field image; and (D) overlap of Hoechst 33342 staining (blue) and NAANPs staining (red); the NAANPs were excited with 405 nm and Hoechst 33342 with UV. (For interpretation of the references to color in this figure legend, the reader is referred to the web version of this article.)

It also confirmed the successful conjugation of NMM to the K^+-stabilized G-quadruplex in the NAANPs [16,17], which provided the prerequisite for cell imaging and therapy.

3.2. Cell imaging using the NAANPs

Owing to its favorable spectroscopic properties, NAANPs should suitably be used as a fluorescent probe for cell imaging. As depicted in part B of Fig. 1, NAANPs was tested to target to cancer cells (e.g. HeLa cells) for fluorescence imaging based on the specific interaction between AS1411 and the nucleolin over-expressed on the cancer cell surface. In the experiment, HeLa cells were stained with a 10 nM NAANPs in PBS buffer (pH 7.4) containing 100 mM KCl for 1 h at 37 °C and 5% CO_2, followed by image acquisition via LSCM. As illustrated in Fig. 4B D, significant homogeneously red fluorescence could be observed on the cell surface. Imaging results with the NAANPs were reproducible for the HeLa cells. By comparing the phase-contrast image with Hoechst 33342 nuclear staining (Fig. 4A), it was found that the NAANPs were mainly bound on the cell membrane. In addition, no fluorescence imaging was observed for HeLa cells treated with citric acid-templated gold nanoparticles at the same conditions as NAANPs (see Fig. S2). These results demonstrated the easy cellular uptake of the fluorescent NAANPs and successful cell imaging ascribed to the specific interaction between AS1411 aptamer and the nucleolin as well as the fluorescence enhancement of NMM binding to the AS1411 quadruplexes.

To confirm the specificity of the NAANPs for nucleolin over-expressed cancer cell imaging, HEK293 cells was treated with NAANPs at the same conditions as the HeLa cells, followed being scanned for LSCM. As shown in Fig. S3A,B, no obvious fluorescence imaging can be observed, indicating the scarce cellular uptake of the fluorescent NAANPs for HEK293 cells. This was because the normal cells lack or have very lower levels of the nucleolin receptors on the plasma membrane [8], thus less NAANPs could be bound to the normal cells through the specific AS1411-nucleolin interaction. Subsequently, it can be confirmed that such internalization of NAANPs was cell-specific.

To show the effect of the gold nanoparticles, AS1411 combined with NMM (AS1411-NMM) was prepared. Images of HeLa cells incubated with AS1411-NMM at the same conditions as NAANPs were also collected. By comparing the images, it can be seen that due to the gold nanoparticles, the fluorescence of AS1411-NMM treated cells (Fig. S3C,D) was much weaker than that of NAANPs. It showed that gold nanoparticles herein played the role not only as the carrier, but also as an enhancer for increasing the uptake of AS1411-NMM onto the cells [28]. As a result, effective cell imaging as well as further therapy can be ensured.

3.3. PDT experiment

As designed in part B of Fig. 1, due to the NMM contained in the NAANPs, exposure to white light could produce cytotoxic ROS for cancer cell treatment. To test the PDT effect of the NAANPs, electric torch with white light were applied to illuminate each NAANPs-

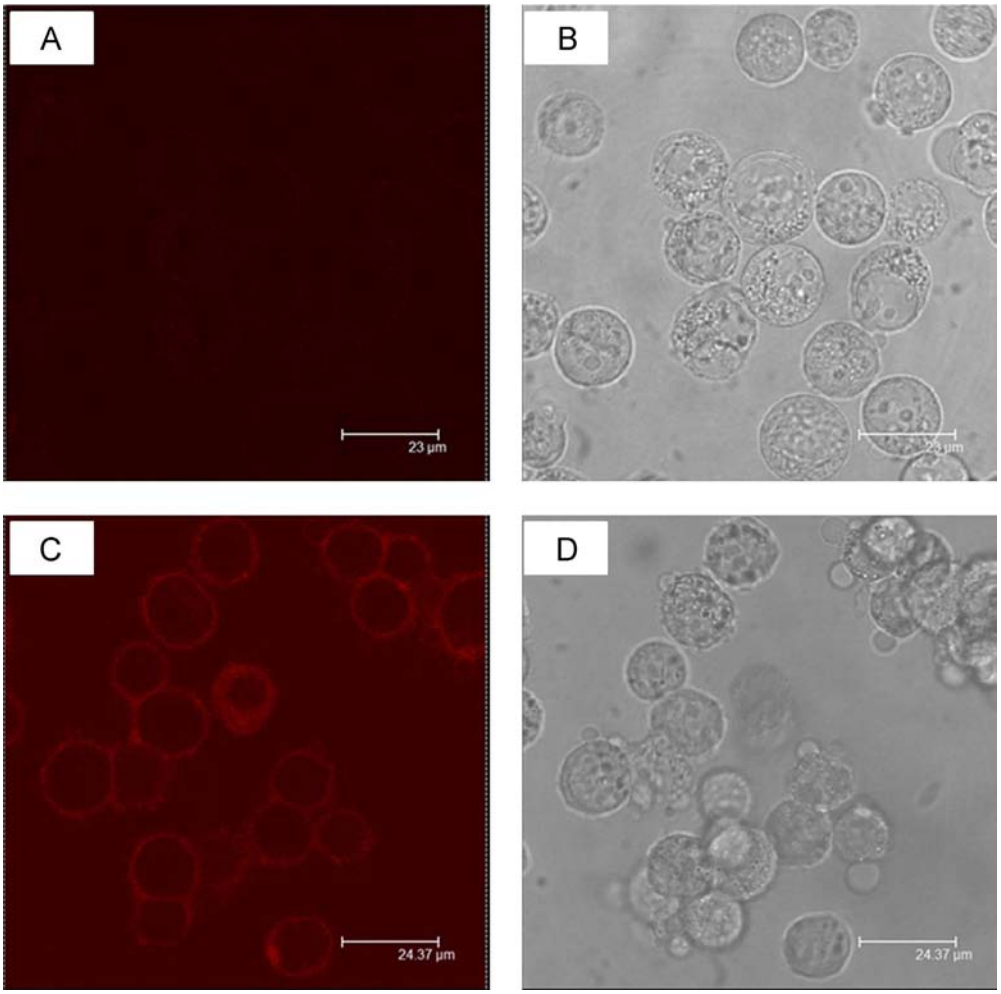

Fig. 5. Cell viability of HeLa cells ($n=8$, mean ± S.D.) after being treated with various concentrations of NAANPs (0, 1, 2, 5, 10 and 20 nM, respectively) (left) and additionally being exposed to light illumination for 30 min (right). Untreated cells without the radiation were severed as the control, of which the viability was set as 100%.

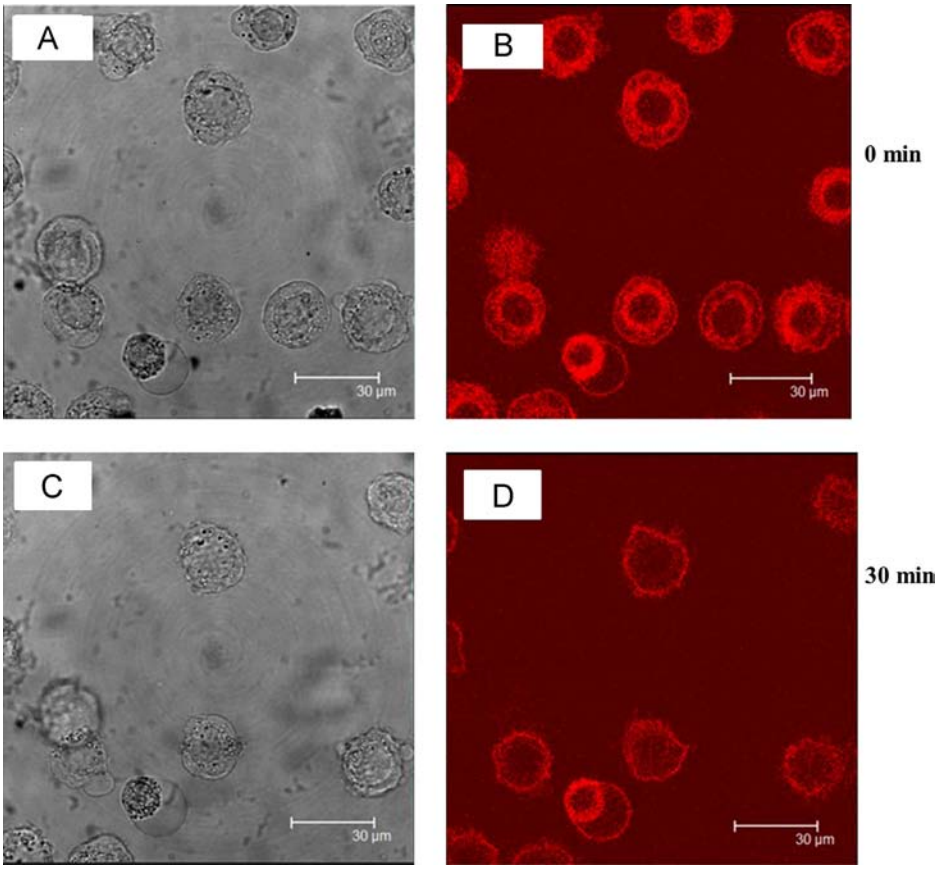

Fig. 6. LSCM images of HeLa cells incubated with 10 nM NAANPs for 1 h at 37 °C (A,B) before and (C,D) after 30 min light irradiation (A,C) bright field images; (B,D) fluorescence images. Excitation wavelength for both was set at 405 nm.

treated cell sample for 30 min, respectively. The illuminated cell samples were then used for further MTT assays and LSCM imaging. To characterize the light source, 1830-C Optical Power Meter (Newport Corp., USA) was used to detect the light intensity. As can be seen in Fig. S4, the emission spectra centered at 455 nm and 550 nm, which were in the white light range of 400–700 nm. Moreover, it was obtained that the light intensity was 12 mW cm^{-2}. It confirmed the feasibility of the electric torch to be used in the PDT experiment.

Firstly, MTT assay was carried out to show the cytotoxicity of NAANPs and the PDT proposal on the HeLa cells. Various concentrations of NAANPs were used to treat the cells. The NAANPs-treated cells with or without the exposure to white light radiation have been studied, respectively. Untreated cells without the radiation were severed as the control, of which the viability was set as 100%. Fig. 5 shows the results of the MTT assay: the cell viability decreased after treatment with the NAANPs and light illumination. The loss of the cell viability increased with the increasing concentrations of the NAANPs in the range of 1–10 nM for both without and with illumination. And a maximum of loss of cell viability was obtained at NAANPs concentration of 10 nM. It should be due to saturated intracellular uptake of NAANPs at higher concentration than 10 nM. However, the NAANPs-treated cells without illumination showed only 14% loss of viability at most. While for the NAANPs-treated cells with illumination, they all exhibited much more obvious loss of viability than that treated with equivalent concentration of NAANPs but no illumination. More than 30% loss of viability could be obtained for the NAANPs-treated cells after light illumination because the photosensitization of NMM attached in the NAANPs could produce cytotoxic ROS to the cells. These results indicated that NAANPs exhibited a little cytotoxicity to HeLa cells by itself, but the white light illumination promoted much more obvious cellular toxicity. As a result, PDT effect to the HeLa cells could be realized.

Moreover, LSCM imaging was also performed to confirm the PDT effect of the NAANPs. As shown in Fig. 6A,B, significant red fluorescence was observed for NAANPs-treated HeLa cells as control. After being placed without further handling, no significant change was obtained for the LSCM imaging. While after being further illuminated for 30 min, the same area of the same cell sample was again scanned to collect the images. It can be seen that the cell amount decreased and the fluorescence of existing cell became much weaker than that before illumination (Fig. 6C,D). This should because after the irradiation of the photosensitizer NMM contained in the NAANPs, it produced cytotoxic ROS to the cells, which was a common phenomenon for porphyrin derivative to induce cell death under light irradiation [19,20]. Accordingly, part of the cell membrane and nuclear of the cells disappeared after the PDT treatment. As a result, fewer cells and lower fluorescence intensity of the left cells could be observed. Thus, both targeted cell imaging and efficient PDT were realized based on the functionalized NAANPs.

4. Conclusions

In conclusion, one multifunctional fluorescent gold nanoparticles (named NAANPs) was synthesized by functionalizing the gold nanoparticles with AS1411 aptamer and then bound with NMM for further targeted cell imaging and PDT. NAANPs could target to the HeLa cells through the specific interaction between the AS1411 aptamer and nucleolin over-expressed on the cell surface.

Fluorescence study confirmed that the fluorescence intensity of NMM could be enhanced significantly upon binding to AS1411 G-quadruplex, thus the NAANPs could be used as appropriate fluorescence reagent for cell imaging. Meanwhile, LSCM and MTT assay gave evidence that NMM could be used as one photosensitizer, thus irradiation of the NAANPs by the white light from a common electric torch could lead to efficient production of cytotoxic ROS to cancer cells, and then a new type of PDT could be established. Specificity of NAANPs was studied by both TEM and LSCM techniques. Gold nanoparticles herein acted as both carrier of the functional groups and enhancer of the fluorescent groups onto the cells, while UV and TEM confirmed that the structures of the gold nanoparticles were not greatly influenced by the functionalization. In addition, gold nanoparticles not only possessed inherently certain cytotoxicity to the cancer cells, but also boosted the cellular uptake of the fluorescent groups. As a result, the efficiency of NAANPs for both the targeted cell imaging and PDT could be ensured.

Furthermore, the proposed method can not only be used as a qualitative method to recognize the presence or absence of the cancer cells, but also has the potential to be used as a semi-quantitative way to indentify the amount of the cancer cells according to the fluorescence of the cell imaging. Compared with some previous works [29,30], the proposed way herein is with advantages of simpleness, cost-effectiveness, etc. It can be anticipated that the multifunctional gold nanoparticles will bring breakthroughs to cancer monitoring, diagnosis, and treatment. It was also predicted that exploiting new functions of existing nanomaterial will extend their applications in bioanalysis.

Acknowledgments

This work was supported by the National Natural Science Foundation of China (Grant nos. 21190040 and 21305133) and 973 projects 2010CB933600, and Jilin Province Science and Technology Development Plan Project (No. 201201006), and the Instrument Developing Project of the Chinese Academy of Sciences (No. YZ201203)

Appendix A. Supplementary material

Supplementary data associated with this article can be found in the online version at http://dx.doi.org/10.1016/j.talanta.2013.09.062.

References

[1] X. Huang, I.H. El-Sayed, W. Qian, M.A. El-Sayed, Nanomedicine 2 (2007) 681–693.
[2] J.A. Barreto, W. O'Malley, M. Kubeil, B. Graham, H. Stephan, L. Spiccia, Adv. Mater. 23 (2011) H18–H40.
[3] C.J. Murphy, A.M. Gole, J.W. Stone, P.N. Sisco, A.M. Alkilany, E.C. Goldsmith, S.C. Baxter, Acc. Chem. Res. 41 (2008) 1721–1730.
[4] E.C. Dreaden, A.M. Alkilany, X. Huang, C.J. Murphy, M.A. El-Sayed, Chem. Soc. Rev. 41 (2012) 2740–2779.
[5] E. Boisselier, D. Astruc, Chem. Soc. Rev. 38 (2009) 1759–1782.
[6] C.R. Patra, R. Bhattacharya, D. Mukhopadhyay, P. Mukherjee, J. Biomed. Nanotechnol. 4 (2008) 99–132.
[7] L.Q. Chen, S.J. Xiao, L. Peng, T. Wu, J. Ling, Y.F. Li, C.Z. Huang, J. Phys. Chem. B 114 (2010) 3655–3659.
[8] C.R. Ireson, L.R. Kelland, Mol. Cancer Ther. 5 (2006) 2957–2962.
[9] S. Soundararajan, W. Chen, E.K. Spicer, N. Courtenay-Luck, D.J. Fernandes, Cancer Res. 68 (2008) 2358–2365.
[10] J. Guo, X. Gao, L. Su, H. Xia, G. Gu, Z. Pang, X. Jiang, L. Yao, J. Chen, H. Chen, Biomaterials 32 (2011) 8010–8020.
[11] A. Aravind, P. Jeyamohan, R. Nair, S. Veeranarayanan, Y. Nagaoka, Y. Yoshida, T. Maekawa, D.S. Kumar, Biotechnol. Bioeng. 109 (2012) 2920–2931.
[12] J. Zhu, L. Zhang, E. Wang, Chem. Commun. 48 (2012) 11990–11992.
[13] T.B. Melo, G. Reisaeter, Biophys. Chem. 25 (1986) 99–104.
[14] T. Li, E. Wang, S. Dong, Anal. Chem. 82 (2010) 7576–7580.
[15] L. Zhang, J. Zhu, J. Ai, Z. Zhou, X. Jia, E. Wang, Biosens. Bioelectron. 39 (2013) 268–273.
[16] H. Li, J. Liu, Y. Fang, Y. Qin, S. Xu, Y. Liu, E. Wang, Biosens. Bioelectron. 41 (2013) 563–568.
[17] C. Zhao, L. Wu, J. Ren, X. Qu, Chem. Commun. 47 (2011) 5461–5463.
[18] J. Ai, T. Li, B. Li, Y. Xu, D. Li, Z. Liu, E. Wang, Anal. Chim. Acta. 741 (2012) 93–99.
[19] L. Brancaleon, H. Moseley, Biophys. Chem. 96 (2002) 77–87.
[20] G. Obaid, I. Chambrier, M.J. Cook, D.A. Russell, Angew Chem. Int. Ed. 51 (2012) 6158–6162.
[21] N. Nombona, K. Maduray, E. Antunes, A. Karsten, T. Nyokong, J. Photochem. Photobiol. B 107 (2012) 35–44.
[22] C. Lim, J. Shin, Y. Lee, J. Kim, H. Park, I.C. Kwon, S. Kim, Small 7 (2011) 112–118.
[23] J.J. Storhoff, R. Elghanian, R.C. Mucic, C.A. Mirkin, R.L. Letsinger, J Am. Chem. Soc. 120 (1998) 1959–1964.
[24] G. Frens, Nat. Phys. Sci. 241 (1973) 20–22.
[25] J.W. Liu, Y. Lu, Angew Chem. Int. Ed. 45 (2006) 90–94.
[26] W. Haiss, N.T.K. Thanh, J. Aveyard, D.G. Fernig, Anal. Chem. 79 (2007) 4215–4221.
[27] J. Li, X. Zhong, F. Cheng, J.-R. Zhang, L.-P. Jiang, J.-J. Zhu, Anal. Chem. 84 (2012) 4140–4146.
[28] S. Khan, F. Alam, A. Azam, A.U. Khan, Int. J. Nanomed. 7 (2012) 3245–3257.
[29] X. He, J. Ge, K. Wang, W. Tan, H. Shi, C. He, Talanta 76 (2008) 1199–1206.
[30] J. Weng, X. Song, L. Li, H. Qian, K. Chen, X. Xu, C. Cao, J. Ren, Talanta 70 (2006) 397–402.